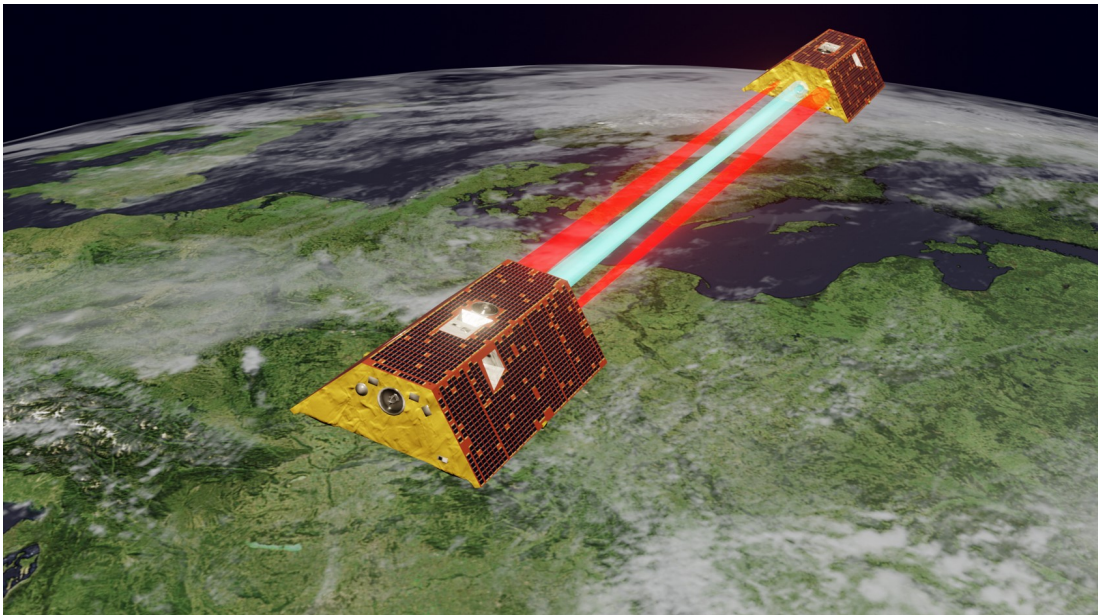




Abstract [GSTM2024-70](#)

Recent Analyses with Alternative LRI1B Datasets of AEI

by [Laura Müller](#), Vitali Müller, Yihao Yan, Malte Misfeldt, Pallavi Bekal, and Gerhard Heinzl





Scan Me

Overview

- AEI LRI1B v54 is available for all month where LRI was able to track (June 2018 – June 2023)
- Sub-release 2024-09-01 is available with 0.5 Hz and 0.2 Hz sampling
- 0.2 Hz dataset is produced by using the KBR CRN filter, to allow easier comparisons of the two ranging instruments
- Range rates in new datasets improved relative to previous AEI releases (around 10 mHz by at least a factor of 2)
- Datasets available at: <https://www.aei.mpg.de/grace-fo-ranging-datasets>

AEI LRI1B
v54

Overview

- AEI LRI1B v54 is available for all month where LRI was able to track (June 2018 – June 2023)
- Sub-release 2024-09-01 is available with 0.5 Hz and 0.2 Hz sampling
- 0.2 Hz dataset is produced by using the KBR CRN filter, to allow easier comparisons of the two ranging instruments
- Range rates in new datasets improved relative to previous AEI releases (around 10 mHz by at least a factor of 2)
- Datasets available at: <https://www.aei.mpg.de/grace-fo-ranging-datasets>

AEI LRI1B
v54

Investigations of Residual Patterns
in official LRI1B v04

Comparison to LRI1B v04

Geographic
Domain



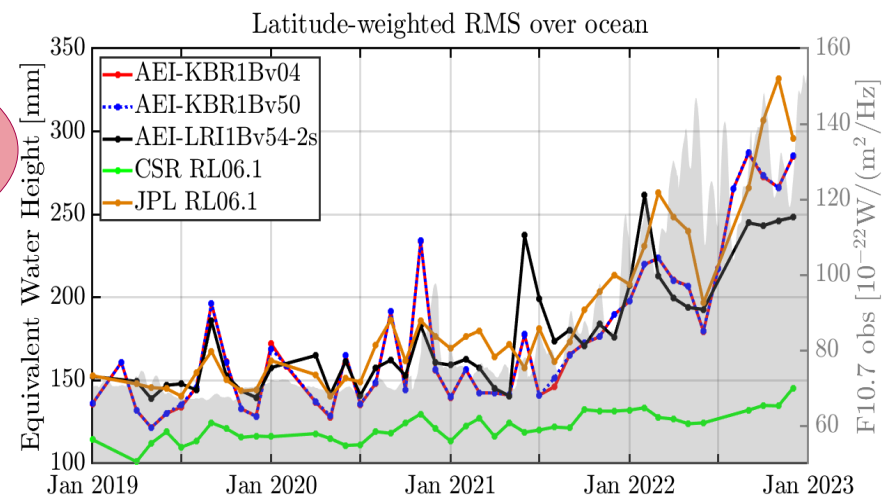
Scan Me



Overview

- Some groups reported that gravity fields from LRI exhibit slightly higher ocean RMS compared to KBR
- Also observed by AEI (black curve higher than blue or red), by using the Chinese gravity field recovery software GSOFT, developed at APM in Wuhan
- Differences between KBR and LRI are usually smaller than KBR solution differences between different processing centers (e.g. CSR/JPL/GFZ)

AEI LRI1B
v54



Overview

- Some groups reported that gravity fields from LRI exhibit slightly higher ocean RMS compared to KBR
- Also observed by AEI (black curve higher than blue or red), by using the Chinese gravity field recovery software GSOFT, developed at APM in Wuhan
- Differences between KBR and LRI are usually smaller than KBR solution differences between different processing centers (e.g. CSR/JPL/GFZ)

We will show some results to support the ongoing investigations.

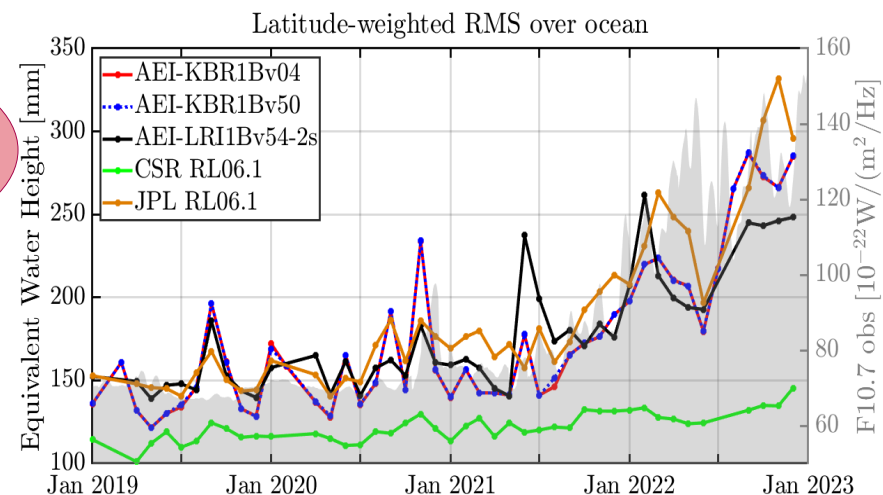
AEI LRI1B v54

Comparison to KBR1B v04

Time Domain

Frequency Domain

Geographic Domain





Re-visiting Results from Duwe et al

- Duwe et al. found different patterns in LRI post-fit residuals when processing the official SDS LRI1B v04.
GSTM2024-75: Poster | Wednesday, 09 Oct, 16:00–17:30

- Two of them appear in Argument of Latitude plots as:
 - Mesh patterns
 - Elliptical rings

- Remark:
 LRI CNR values in v04 are calculated with an incorrect formula.
 Actual CNR is not worse where elliptical rings appear.

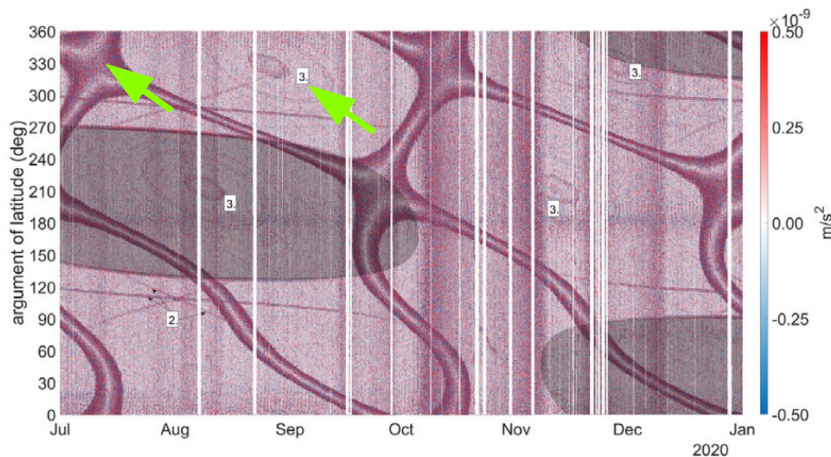


Fig. 4. (b) LRI post-fit range acceleration residuals



Available online at www.sciencedirect.com

ScienceDirect

Advances in Space Research xxx (xxxx) xxx

ADVANCES IN
SPACE
RESEARCH
(a COSPAR publication)
www.elsevier.com/locate/asr

Residual Patterns in GRACE Follow-On Laser Ranging Interferometry Post-Fit Range Rate Residuals

Mathias Duwe*, Igor Koch, Jakob Flury

Leibniz University Hannover, Schneiderberg 50, Hannover, 30167 Hannover, Germany

Received 14 December 2023; received in revised form 12 March 2024; accepted 14 March 2024

Abstract

The novel laser ranging interferometer (LRI) on GRACE Follow-On (GRACE-FO) provides range and range rate measurements for more than 4 years now. Since the launch of the GRACE-FO mission there were few investigations about this measurement system on the level of gravity field recovery and analysis of post-fit residuals. We applied techniques such as along-orbit-analysis or time-argument of latitude diagrams (TAL) to analyse the post-fit range rate residuals as well as the post-fit range acceleration residuals to identify unknown characteristics and systematic effects. The effects are the range rate effect, the panel effect, the Carrier-To-Noise Ratio (CNR) effect and the polar effect. The range rate effect occurs, when the range rate observation $\dot{\rho}$ of the LRI is around 0 m/s. In the TAL diagram the effect appears as a mesh pattern. The panel effect shows patterns of increased residuals when a specific satellite panel starts or stops being illuminated by the Sun. Increased residuals appear when the laser beam is aligned with the Sun. A CNR drop as well as a fluctuation of the yaw and pitch pointing angles obtained from the LRI steering mirrors is observable. Additionally, when the satellites flying into or out of the Earth shadow this effect coincides with the shadow transition effect. Another effect is the CNR effect which appears as an elliptical shape in the TAL diagram. This pattern occurs when the CNR values drop below the LRI requirements of 70 dB-Hz. All these effects have not been detected in the residuals of the GRACE-FO K-band ranging system (KBR) and therefore further investigation and studies will improve the understanding and applications of LRI technology.

© 2024 COSPAR. Published by Elsevier B.V. This is an open access article under the CC BY license (<http://creativecommons.org/licenses/by/4.0/>).

Keywords: GRACE Follow-On; Laser ranging; LRI; Post-fit residuals; Gravity field

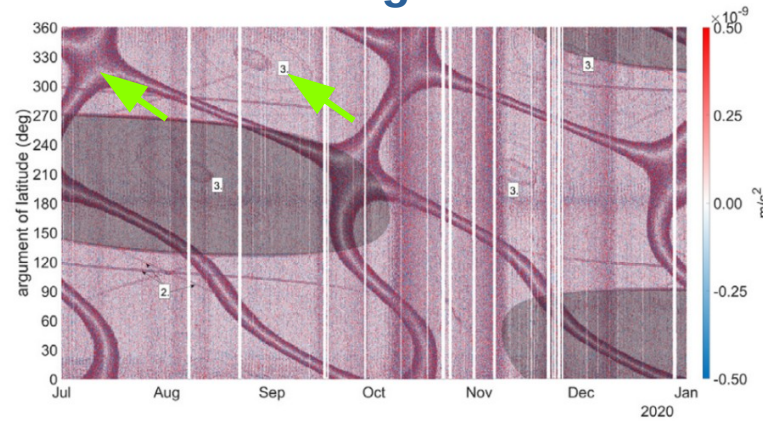




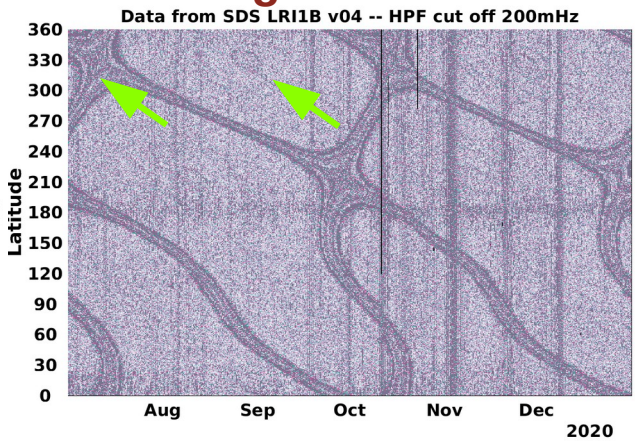
Re-Analysis of LRI Residual Patterns

- We were able to confirm these features by computing post-fit residuals from LRI1B v04 data
- AEI in-house derived LRI1B v54 does not show this features
- Diagonal lines in right plot are most likely caused by empirical parameter estimation

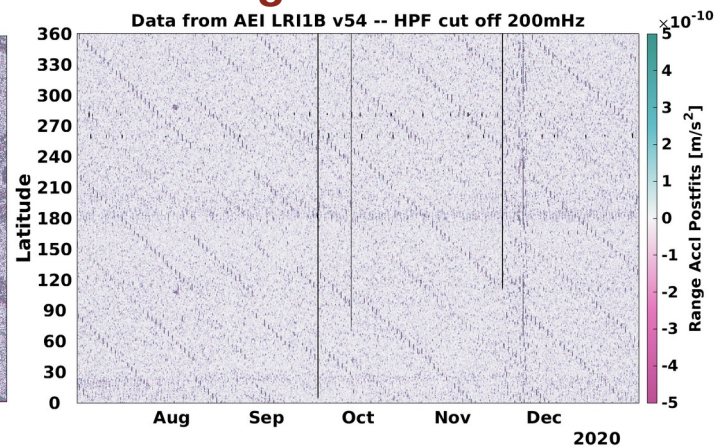
Duwe et al¹ using LRI1B of SDS



AEI using LRI1B of SDS



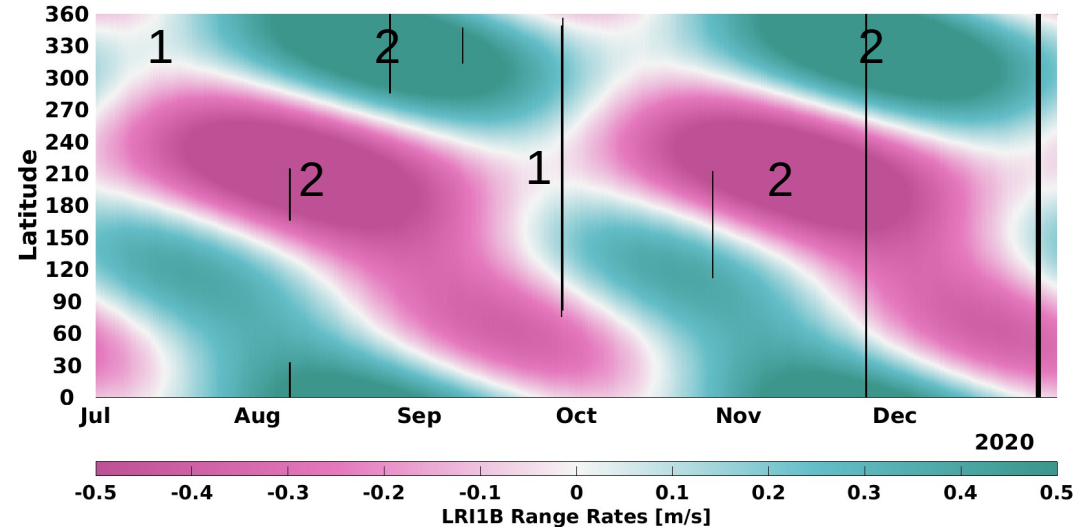
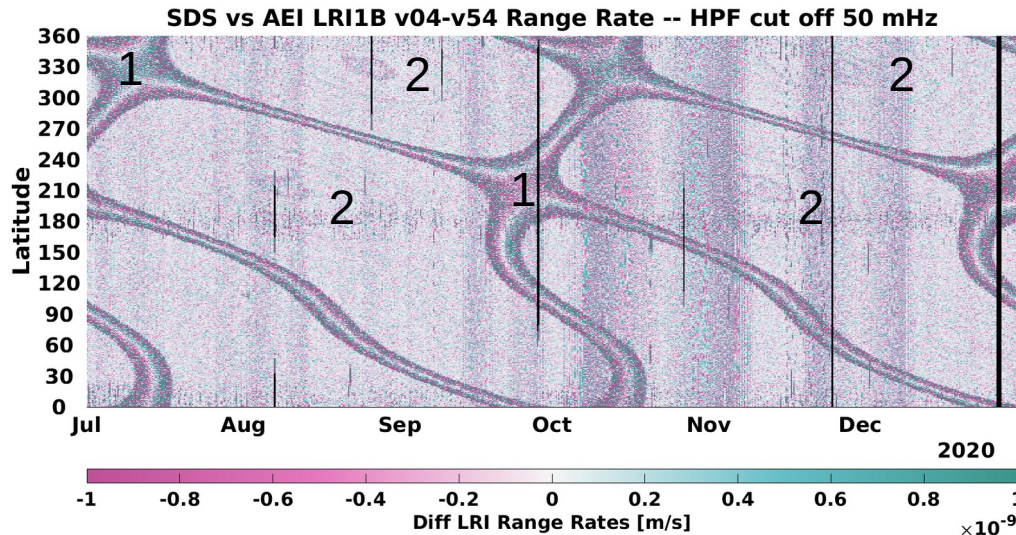
AEI using in-house LRI1B





Residual Patterns already in LRI1B

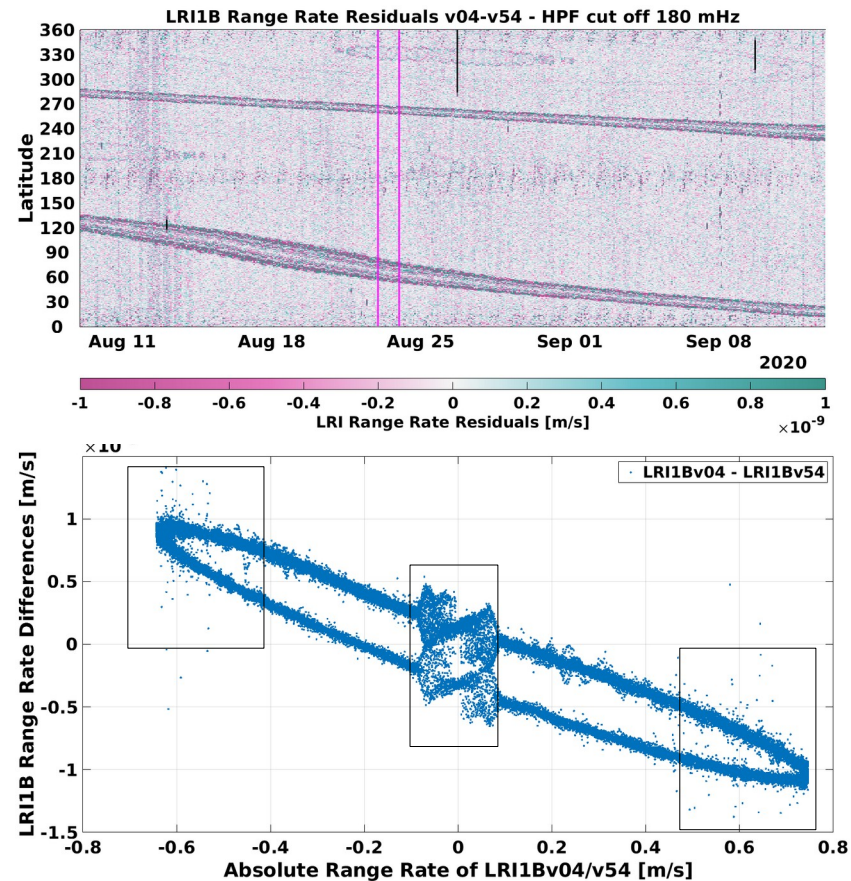
- Comparing LRI1B v04-v54 high-pass filtered biased ranges, range rates or range acccl (without light time correction) show the same features.
- Effects occur when range rate gets
 - 1) close to zero (mesh pattern)
 - 2) close to max or minimum (elliptical rings)





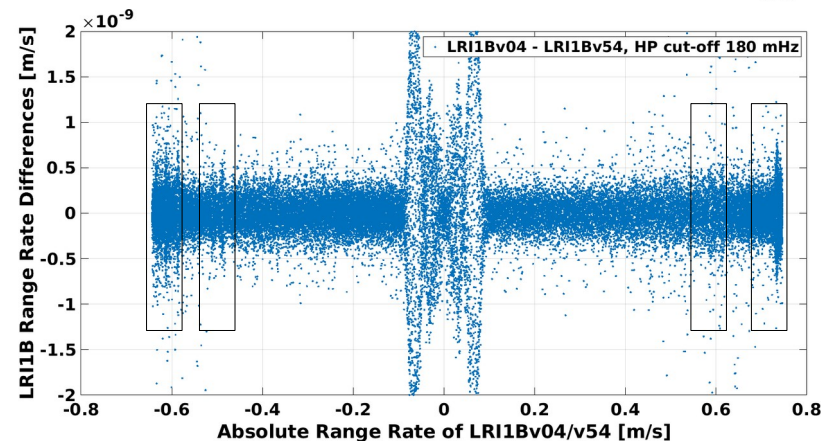
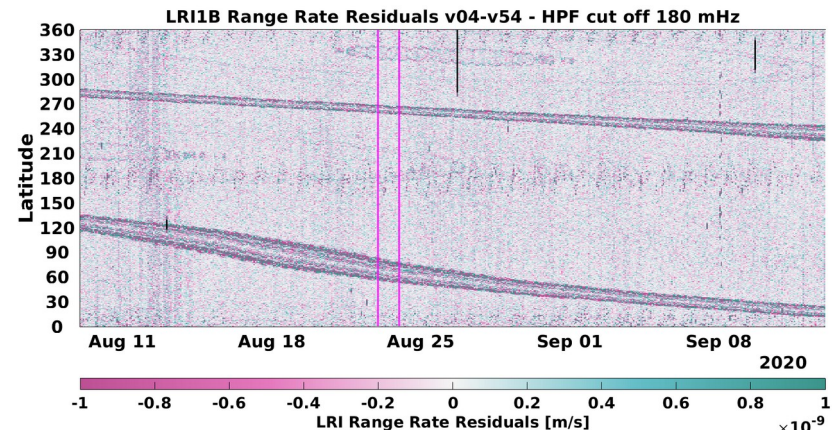
Correlation between Residuals and Range Rates

- 2020-08-23 contains zero crossings and elliptical rings
- LRI1B residuals (not filtered) over range rates show:
 - ellipse, due to different scale and time shift
 - clustering around 0 m/s
 - outliers at minimal and maximal range rates



Artifacts at Particular Range Rate Values

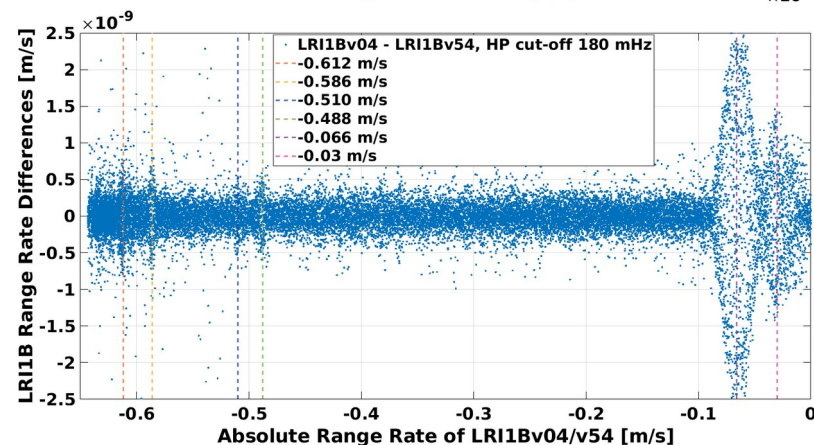
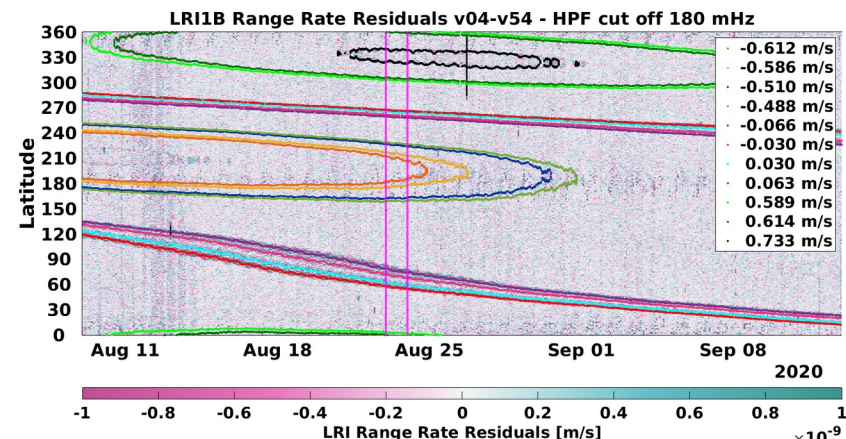
- 2020-08-23 contains zero crossings and elliptical rings
- LRI1B residuals (not filtered) over range rates show:
 - ellipse, due to different scale and time shift
 - clustering around 0 m/s
 - outliers at minimal and maximal range rates
- High-pass filtered LRI1B residuals over range rates makes it easier to identify cluster at certain range rates



Artifacts at Particular Range Rate Values

- 2020-08-23 contains zero crossings and elliptical rings
- LRI1B residuals (not filtered) over range rates show:
 - ellipse, due to different scale and time shift
 - clustering around 0 m/s
 - outliers at minimal and maximal range rates
- High-pass filtered LRI1B residuals over range rates makes it easier to identify cluster at certain velocities
- Clustering observed at range rates, where the signatures in Argument of Latitude plots appear.

→ Not clear why effect appears in official LRI1B v04





Checking LRI1A v04 data

We performed analysis if v04 LRI1A data might already contain artifacts related to particular absolute range-rate values.

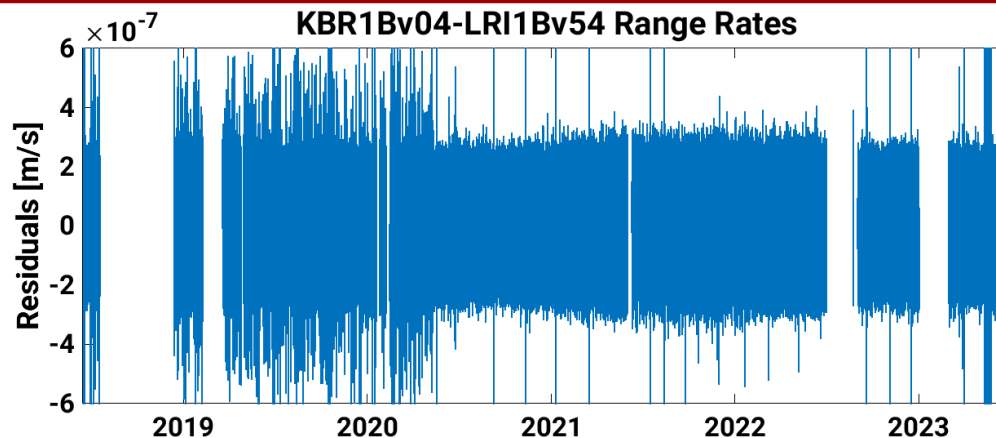
- Our hypotheses were that artifacts might be caused by
 - piston phase quantity, which has lower numerical accuracy than the raw individual phase values (double floating point vs. unsigned integer 64-bit)
 - loss of precision in the time-tag values (rounded to nanosecond in LRI1A)
- Neither hypothesis was supported by the data (some plots are shown in the back-up slides below)
 - v04 LRI1A data seems not to be affected by artifacts at particular range rates
 - artifacts / signatures probably introduced in v04 L1A-> L1B processing



KBR & LRI Residuals in Time Domain

KBR1B v04 – LRI1B v54 Range Rate Residuals are dominated by

- high frequency noise
 - from KBR phase readout approx. $\pm 0.3 \mu\text{m/s}$
 - 2018 – March 2020 several peaks most likely related to outlier in CLK1B





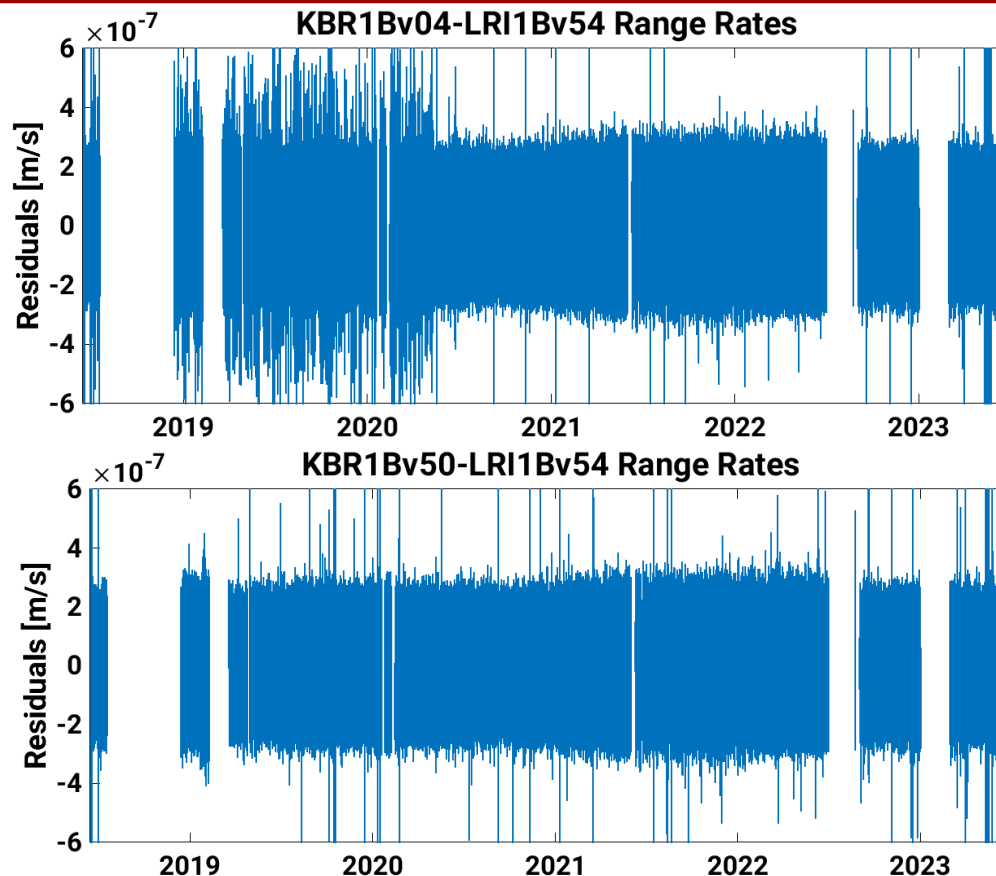
KBR & LRI Residuals in Time Domain

KBR1B v04 – LRI1B v54 Range Rate Residuals are dominated by

- high frequency noise
 - from KBR phase readout approx. $\pm 0.3 \mu\text{m/s}$
 - 2018 – March 2020 several peaks most likely related to outlier in CLK1B

AEI-KBR1B v50 does not show as many outliers as v04 in the first period.

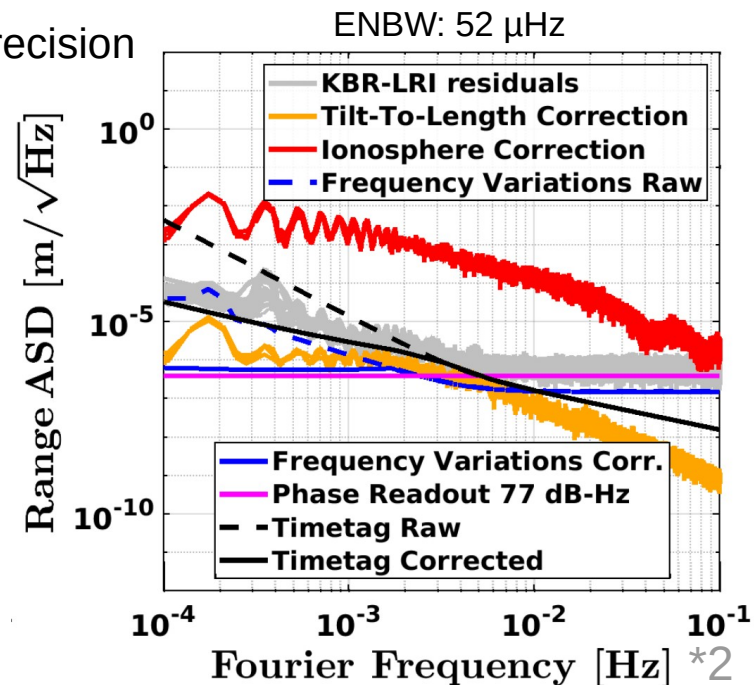
AEI-KBR1B v50 available at
<https://doi.org/10.25625/MCTZKS>
 (Publication in preparation, by Yihao Yan et al.)





KBR & LRI Residuals in Frequency Domain

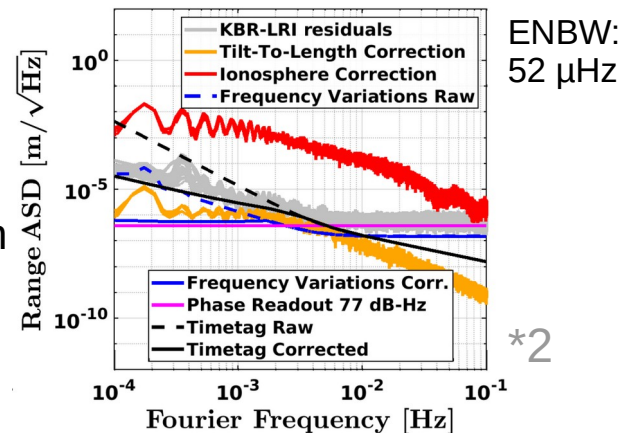
- ASD show KBR-LRI residuals with gray traces for all days in January 2019.
- KBR-LRI residuals seems to be limited at ²
 - high frequencies: by the KBR phase readout noise
 - low frequencies: by time-tag precision determined by the CLK1B precision





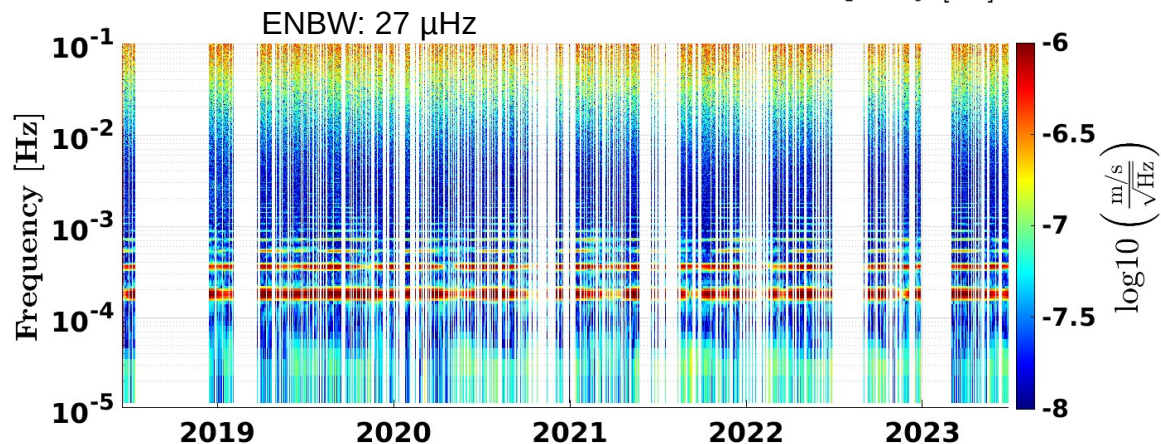
KBR & LRI Residuals in Frequency Domain

- ASD show KBR-LRI residuals with gray traces for all days in January 2019.
- KBR-LRI residuals seems to be limited at ²
 - high frequencies: by the KBR phase readout noise
 - low frequencies: by time-tag precision determined by the CLK1B precision



Daily ASD of range rate residuals between KBR1B v04 and LRI1B v54

- seasonal variations in 1/rev...6/rev frequencies, which are correlated to temperature variations which might couple into the KBR system ³
- 2/rev maximum difference ~5 nm/s rms amplitude (correspond to ~0.013 nm/s²)
- high frequencies above 1 mHz show no obvious features



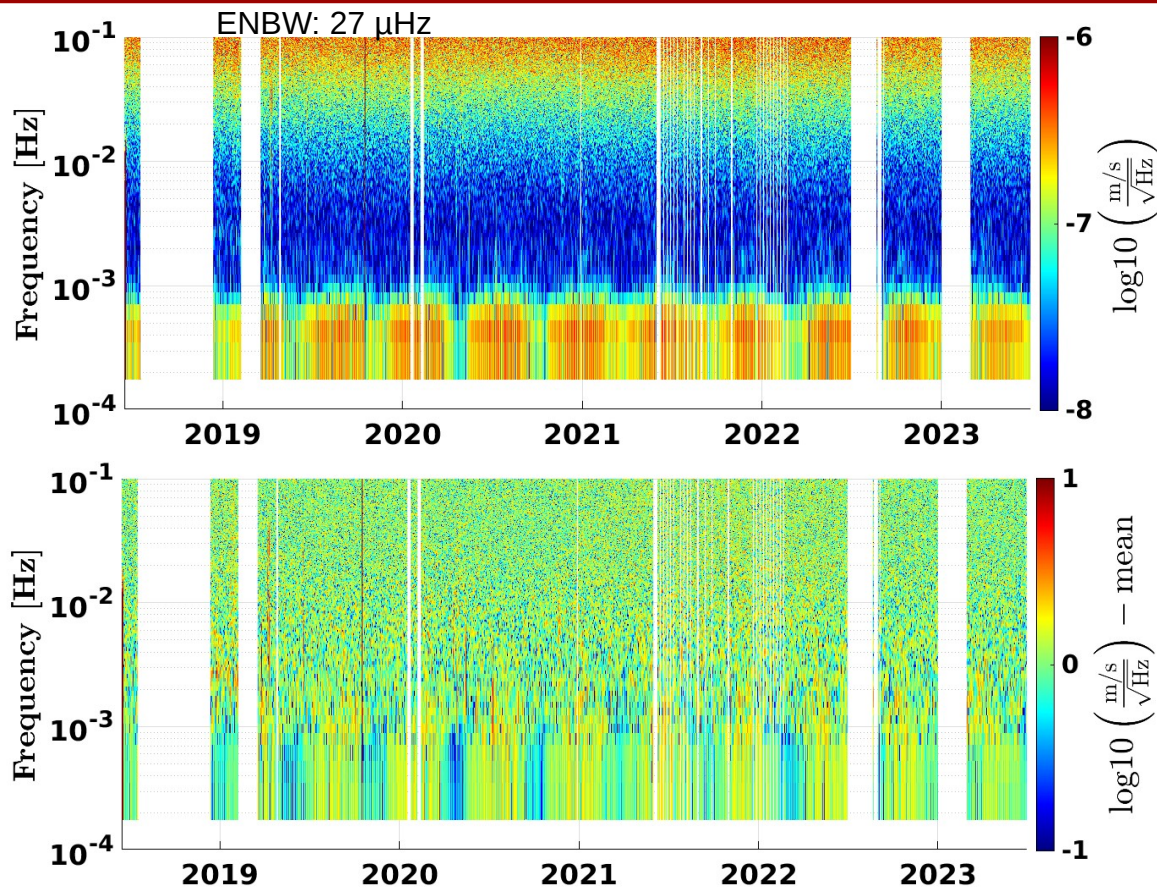
KBR & LRI Residuals in Frequency Domain

Orbit-wise ASD for finer resolution:

- show seasonal variations at n/rev
- high frequencies above 1 mHz show no special patterns

Orbit-wise ASD minus mean value of each frequency bin over complete time span:

- in general noise in residuals relatively similar for whole time span
- few disturbances are visible at:
 - satellite maneuvers like CoM calibrations or thruster plateau tests
 - 2019-10-16/17 with KBR SNR drop,
 - e.g. 2019-05-09, 2019-06-10/11 caused by CLK1B outliers





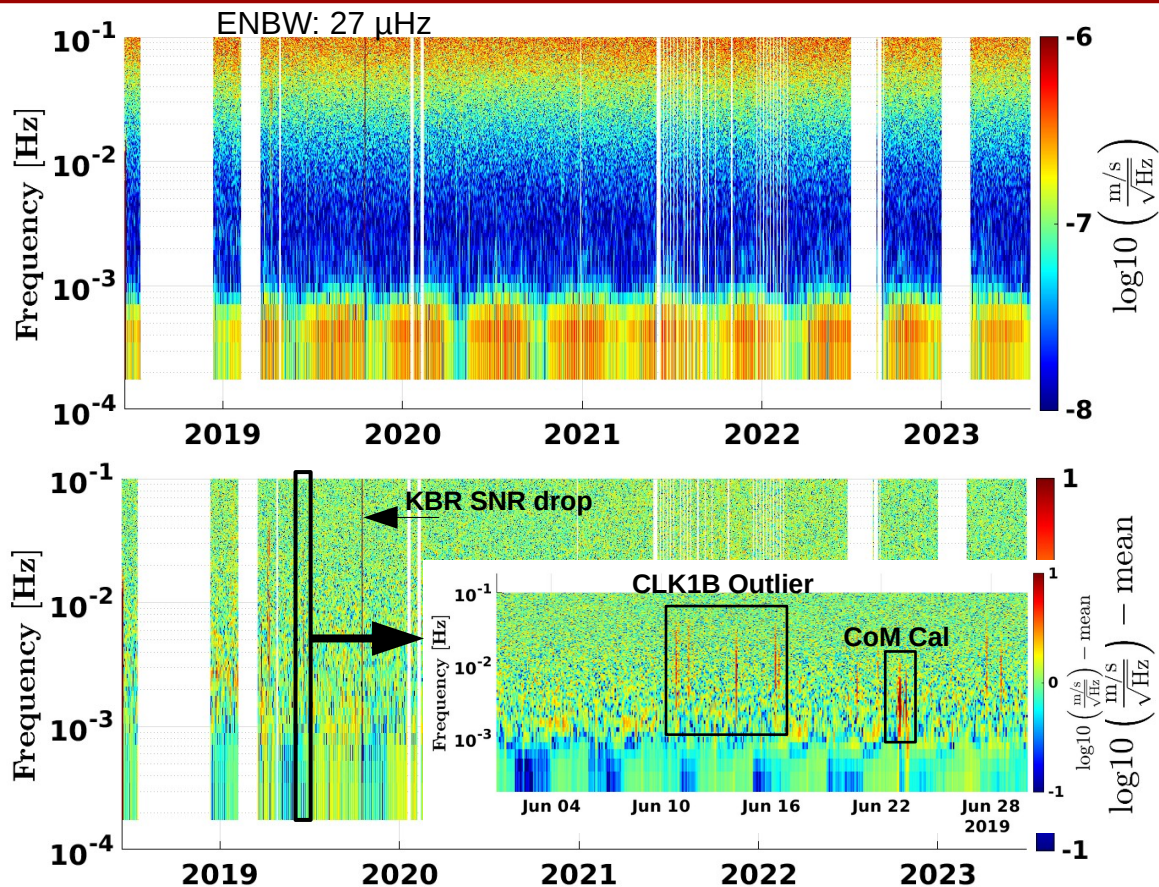
KBR & LRI Residuals in Frequency Domain

Orbit-wise ASD for finer resolution:

- show seasonal variations at n/rev
- high frequencies above 1 mHz show no special patterns

Orbit-wise ASD minus mean value of each frequency bin over complete time span:

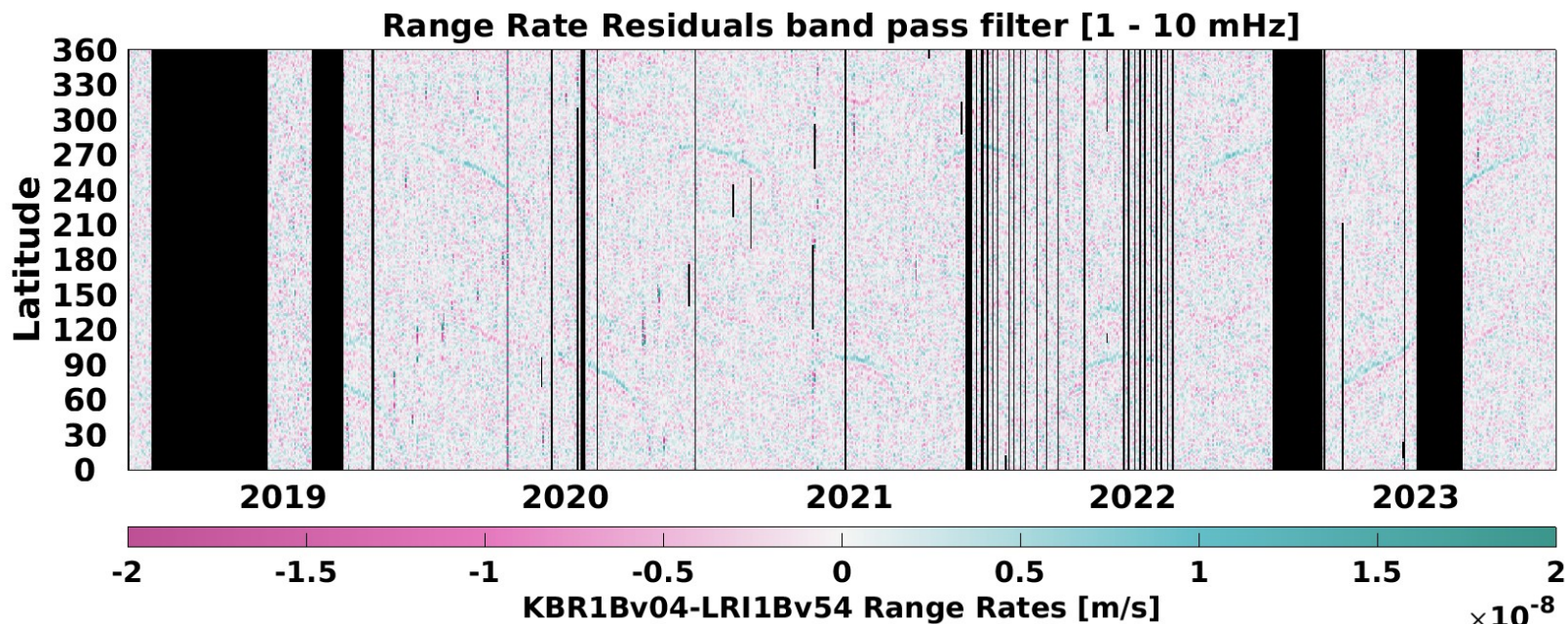
- in general noise in residuals relatively similar for whole time span
- few disturbances are visible at:
 - satellite maneuvers like CoM calibrations or thruster plateau tests
 - 2019-10-16/17 with KBR SNR drop,
 - e.g. 2019-05-09, 2019-06-10/11 caused by CLK1B outliers





KBR & LRI Residuals in Geographic Domain

- Frequencies above 10 mHz dominated by KBR noise
- Here frequency band between 1 mHz and 10 mHz
- shadow transitions are slightly visible
- Otherwise no special differences observable in geographic domain





Conclusion

LRI1B v04 – v54 artifacts related to particular range rate values

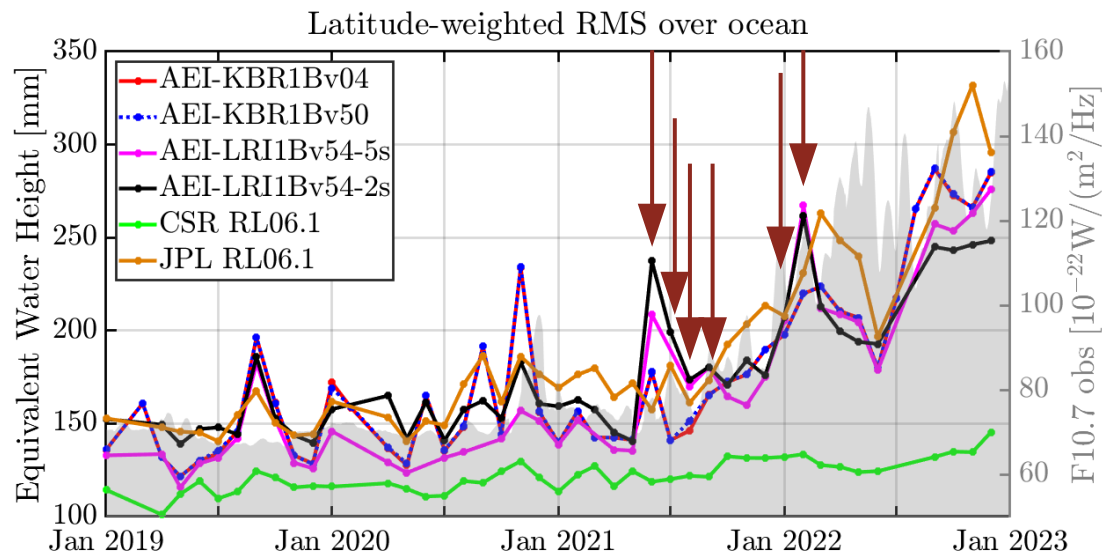
- LRI1B v04 exhibits some artifacts, which are not in AEI-LRI1B v50 & v54
- No evidence found that LRI1A v04 is affected
- Effects couple during L1A → L1B processing

KBR1B v04 – LRI1B v54 Comparison

- KBR1B v04 - LRI1B v54 residuals
 - are dominated by the KBR noise level above 1 mHz
 - show shadow transitions between 1 - 10 mHz in geographic domain
 - show seasonal variations in differences at $1/\text{rev} \dots 6/\text{rev}$ tone-frequencies
- Largest differences, e.g. at $2/\text{rev}$, reach rms amplitudes of ~ 0.5 nm/s (~ 2.6 μm or ~ 0.013 nm/s^2), which might cause differences in the gravity field recovery
- However, we assume that monthly gravity fields from both ranging instruments should still result in (at least) similar values for the ocean RMS.
- AEI provides a LRI1B dataset with 0.2 Hz sampling and KBR CRN filter parameters, to simplify comparison between LRI and KBR and exclude that CRN filter or data rate has an impact..

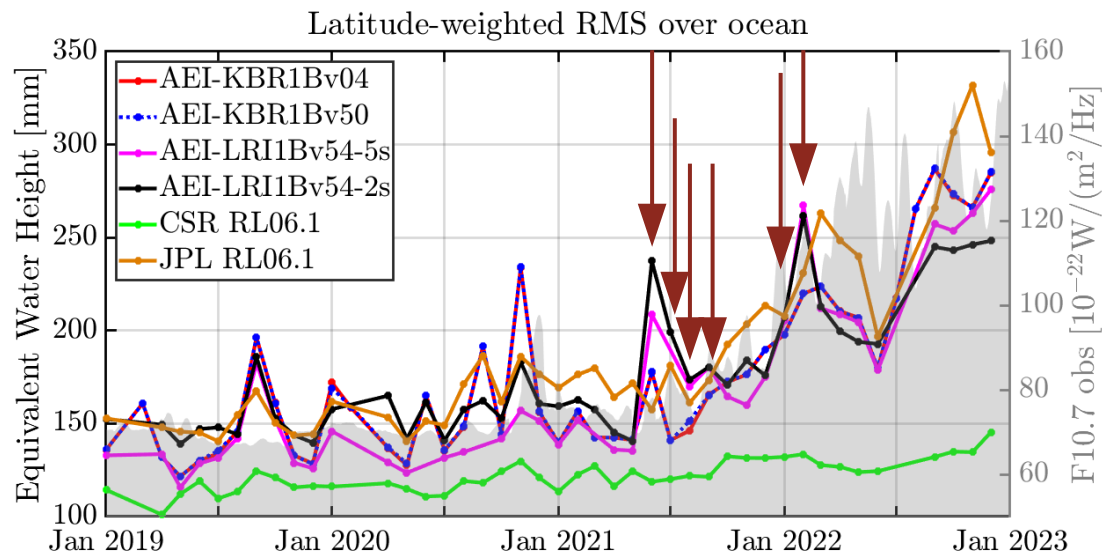
Outlook

- Processing the 0.2 Hz AEI-LRI1Bv54 dataset with GSOFTE, yield lower or equal ocean RMS values for LRI (pink curve), in comparison to KBR (red & blue curve)
- **Exceptions** are month where less LRI data was available, e.g. due to NADIR-pointing (June-September 2021 January & February 2022)



Outlook

- Processing the 0.2 Hz AEI-LRI1Bv54 dataset with GSOFT, yield lower or equal ocean RMS values for LRI (pink curve), in comparison to KBR (red & blue curve)
- **Exceptions** are month where less LRI data was available, e.g. due to NADIR-pointing (June-September 2021 January & February 2022)
- Next Steps:
We need to figure out, how to achieve an optimal LRI Level 2 data processing, and why the sampling rate has an impact on the solutions.



References

- ¹ Mathias Duwe et al 2024, Residual Patterns in GRACE Follow-On Laser Ranging Interferometry Post-Fit Range Rate Residuals, <https://doi.org/10.1016/j.asr.2024.03.035>
- ² Vitali Müller et al, 2022, Comparing GRACE-FO KBR and LRI ranging data with focus on carrier frequency variations, <https://doi.org/10.3390/rs14174335>
- ³ Malte Misfeldt et al. 2022, Scale Factor Determination for the GRACE-Follow On Laser Ranging Interferometer including Thermal Correction, <https://doi.org/10.3390/rs15030570>

Other related references for AEI LRI1B processing:

Laura Müller, 2021, Generation of Level 1 Data Products and Validating the Correctness of Currently Available Release 04 Data for the GRACE Follow-On Laser Ranging Interferometer, Master's thesis, DOI:<http://doi.org/10.15488>

Yihao Yan et al, 2020, Revisiting the Light Time Correction in Gravimetric Missions Like GRACE and GRACE Follow-On, <https://doi.org/10.1007/s00190-021-01498-5>

Henry Wegener, 2020, Tilt-to-Length Coupling in the GRACE Follow-On Laser Ranging Interferometer, <https://doi.org/10.2514/1.A34790>

AEI-LRI1B: <https://www.aei.mpg.de/grace-fo-ranging-datasets>

AEI-KBR1B: <https://doi.org/10.25625/MCTZKS>



Scan Me



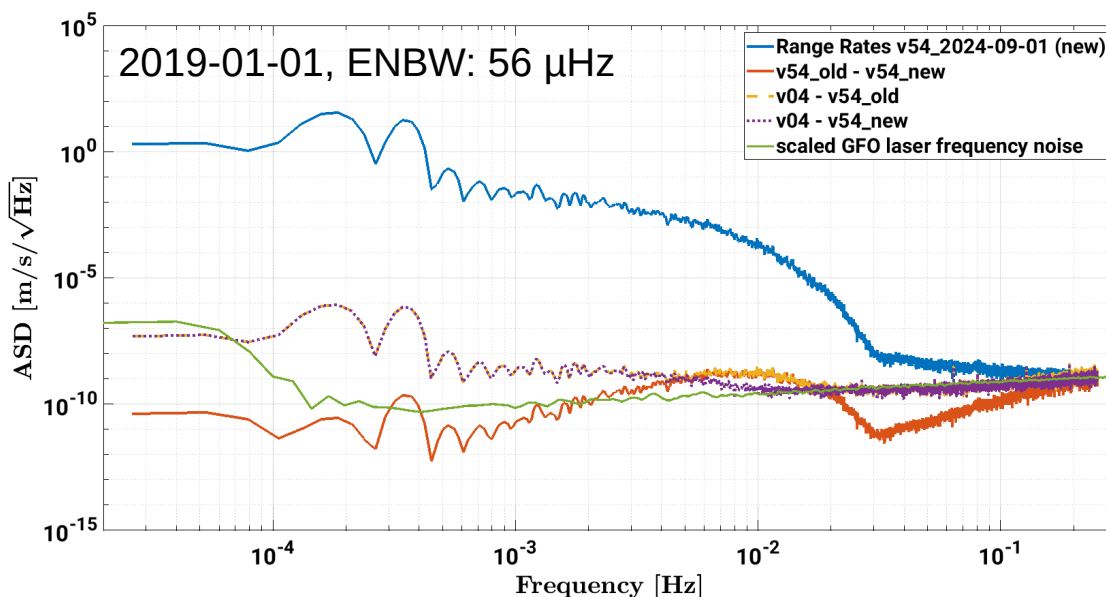
Back Up Slides





LRI1B v54 2024-09-01 Improvement

- Previous method of computing time derivatives on 0.5 Hz rate inserted noise around 10 mHz
- Computing derivatives on 10 Hz rate, with numerical approach or CRN filter, lowers the bump at 10 mHz by at least a factor of 2





Checking LRI1A v04 for certain range rate patterns

- LRI1A provides
 - 1) **raw phase** measurements from four photo-diode channels as uint64 (2x uint32)
 - 2) **mean phase** (piston phase) with double precision → further processed to L1B biased range

LRI1A v04 Format

183 # End of YAML header

```

184 599572800 64095949 C 0000000111111111 00000000
185 599572800 167572770 C 0000000111111111 00000000
186 599572800 271049591 C 0000000111111111 00000000
187 599572800 374526412 C 0000000111111111 00000000
188 599572800 478003234 C 0000000111111111 00000000
189 599572800 581480055 C 0000000111111111 00000000
190 599572800 684956876 C 0000000111111111 00000000
191 599572800 788433697 C 0000000111111111 00000000
192 599572800 891910518 C 0000000111111111 00000000
193 599572800 995387340 C 0000000111111111 00000000

```

Piston Phase

```

78561638205.90274
78562759128.66217
78563880063.02751
78565001009.00334
78566121966.58719
78567242935.77693
78568363916.57001
78569484908.96179
78570605912.95645
78571726928.54474

```

Channel 0

```

3068813992 1795771311
3068857778 1990287169
3068901564 4131954641
3068945351 3926574460
3068989139 1373725692
3069032927 768026978
3069076715 2109044725
3069120504 1101032145
3069164293 2039659136
3069208083 628409030

```

Channel 1

```

3068813992 1795477384
3068857778 1989996250
3068901564 4131664004
3068945351 3926283313
3068989139 1373432695
3069032927 767737480
3069076715 2108751859
3069120504 1100739759
3069164293 2039365509
3069208083 628112846

```

Channel 2

```

3068813992 1795477262
3068857778 1989996235
3068901564 4131664035
3068945351 3926283273
3068989139 1373432765
3069032927 767737528
3069076715 2108751716
3069120504 1100739780
3069164293 2039365497
3069208083 628112884

```

Channel 3

```

3068813992 1795771172
3068857778 1990287307
3068901564 4131954687
3068945351 3926574472
3068989139 1373725633
3069032927 768026776
3069076715 2109044873
3069120504 1101032229
3069164293 2039659176
3069208083 628408899

```

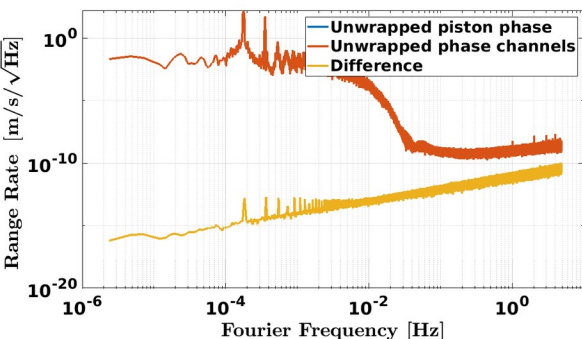




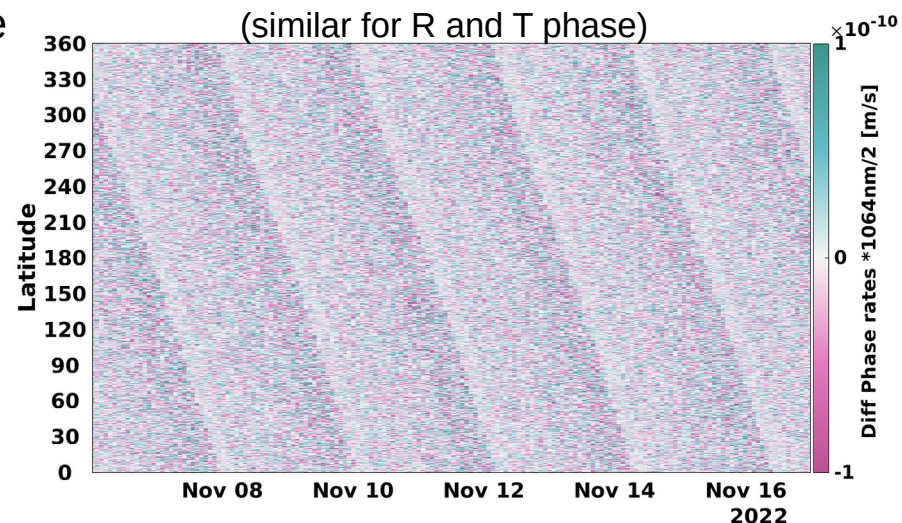
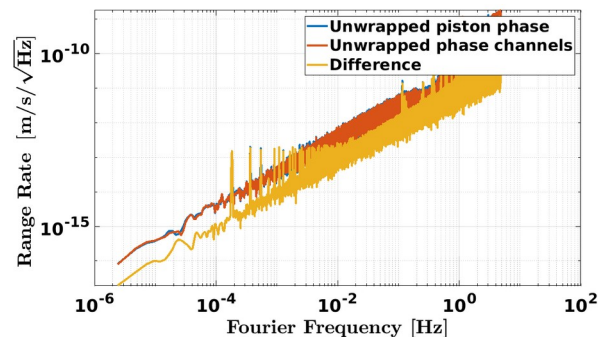
Checking LRI1A v04 for certain range rate patterns

- LRI1A provides
 - 1) raw phase measurements from four photo-diode channels as uint64 (2x uint32)
 - 2) mean phase (piston phase) with double precision → further processed to L1B
- We unwrapped phases of 1) & 2) and plotted their differences
- Piston Phase is less precise, but differences smaller than $1e-10$ m/s and also range rate correlated patterns (like mesh-pattern) cannot be observed
 - LRI1A v04 piston phase most likely not affected

Reference (R)
Phase Rate $\times 1064\text{nm}/2$



Transponder (T)
Phase Rate $\times 1064\text{nm}/2$





Checking LRI1A v04 for certain range rate patterns

- LRI1A v04 time-tags are rounded to nanoseconds, while LRP provides time-tags in femtosecond resolution

LRI1A v04 Format

```

87 - rcv_time:
88   comment: 1st column
89   coverage_content_type: referenceInformation
90   long_name: Seconds past 12:00:00 noon of January 1, 2000 in LRI Time
91   units: seconds
92 - rcvtime_frac:
93   comment: 2nd column
94   coverage_content_type: referenceInformation
95   long_name: Fractional portion of time tag
96   units: nanoseconds
97   valid_range: 0, 999999999

```

GF1 LRP Time-tag example:

Int: 599572800 GrGps sec

Frac: 2477693 clockticks

Clockrate: 38656000 Hz

$$\begin{aligned} \text{rcvtime_frac} &= \text{clockticks} / \text{clockrate} * 1\text{e}9 \\ &= 64095948.8824503 \text{ nanosec} \end{aligned}$$

```

183 # End of YAML header
184 599572800 64095949 C 0000000111111111 00000000 78561638205.90274 3068813992 1795771311 3068813992 1795477384 3068813992 1795477262 3068813992 1795771172
185 599572800 167572770 C 0000000111111111 00000000 78562759128.66217 3068857778 1990287169 3068857778 1989996250 3068857778 1989996235 3068857778 1990287307
186 599572800 271049591 C 0000000111111111 00000000 78563880063.02751 3068901564 4131954641 3068901564 4131664004 3068901564 4131664035 3068901564 4131954687
187 599572800 374526412 C 0000000111111111 00000000 78565001009.00334 3068945351 3926574460 3068945351 3926283313 3068945351 3926283273 3068945351 3926574472
188 599572800 478003234 C 0000000111111111 00000000 78566121966.58719 3068989139 1373725692 3068989139 1373432695 3068989139 1373432765 3068989139 1373725633
189 599572800 581480055 C 0000000111111111 00000000 78567242935.77693 3069032927 768026978 3069032927 767737480 3069032927 767737528 3069032927 768026776
190 599572800 684956876 C 0000000111111111 00000000 78568363916.57001 3069076715 2109044725 3069076715 2108751859 3069076715 2108751716 3069076715 2109044873
191 599572800 788433697 C 0000000111111111 00000000 78569484908.96179 3069120504 1101032145 3069120504 1100739759 3069120504 1100739780 3069120504 1101032229
192 599572800 891910518 C 0000000111111111 00000000 78570605912.95645 3069164293 2039659136 3069164293 2039365509 3069164293 2039365497 3069164293 2039659176
193 599572800 995387340 C 0000000111111111 00000000 78571726928.54474 3069208083 628409030 3069208083 628112846 3069208083 628112884 3069208083 628408899

```





Checking LRI1A v04 for certain range rate patterns

- LRI1A v04 time-tags are rounded to nanoseconds, while LRP provides time-tags in femtosecond resolution
- We computed the LRI phase (transponder-reference phase)
 - from LRI1A v04 piston phase with AEI algorithm
 - from LRI raw phase measurements with AEI algorithm
 After interpolating both sets on the same time-grid, and comparing their difference they do not show the signatures (mesh-patterns or elliptic rings)
- LRI1Av04 time-tags are also not causing the signatures like mesh-patterns or elliptic rings
 - LRI1A v04 most likely not affected, signatures couple during L1A → L1B v04 processing

